

Monolayer formation of PBLG–PEO block copolymers at the air–water interface

Youngmi Park^a, Young-Wook Choi^a, Sangwook Park^a, Chong Su Cho^b, Michael J. Fasolka^c, Daewon Sohn^{a,*}

^a Department of Chemistry, Hanyang University, Seoul 133-791, South Korea

^b School of Agricultural Biotechnology, Seoul National University, Seoul 151-742, South Korea

^c Polymers Division, National Institute of Standard and Technology, Gaithersburg, MD 20899, USA

Received 9 July 2004; accepted 15 September 2004

Available online 11 November 2004

Abstract

Physicochemical properties of PBLG (poly(γ -benzyl-L-glutamate))–PEO (poly(ethylene oxide)) diblock copolymers composed of PBLG as the hydrophobic rod component and PEO as the hydrophilic component were investigated at the air–water interface. Surface pressure–area isotherms obtained by the Wilhelmy plate method provide several variables such as molecular size, compressibility of PEO, and the free energy change of the PBLG–PEO block copolymer. GE-1 (M_w of PBLG:PEO = 103,700:12,000), with a relatively longer rod, has negative temperature effects and GE-3 (M_w of PBLG:PEO = 8400:12,000), with a relatively shorter rod, shows a positive temperature effect because of the large entropy loss. These competitions were based on the block size of PBLG and PEO and were affected by various microstructures of the PBLG–PEO diblock copolymer. Monolayer aggregations transferred onto mica from the air–water interface were analyzed with AFM. AFM images of GE-1 monolayers show cylindrical micelles, but the self-assembled structure has many large domains. The monolayer of GE-2 (M_w of PBLG:PEO = 39,800:12,000), which has a medium size rod, forms a spherical structure at the air–water interface. Monolayers of GE-3, with a short rod length, form bilayer structures. These results demonstrate that the microstructures of PBLG–PEO diblock copolymers are related to free energy changes between rod and coil blocks.

© 2004 Elsevier Inc. All rights reserved.

Keywords: PBLG–PEO; Langmuir–Blodgett; Compressibility; Block copolymer; Surface pressure

1. Introduction

Rod–coil molecules consisting of a rigid rod block and a flexible coil block are a novel type of block copolymer with a unique microstructural organization held together by noncovalent forces including hydrophobic and hydrophilic effects, electrostatic interactions, and hydrogen bonding. These forces control the phase behavior of these rod–coil molecules. Formation of anisotropic structures is the main factor in the microphase separation of the coil and rod blocks. Rodlike molecules have been widely studied. They

exhibit liquid crystalline ordered phases such as nematic and/or layered smectic types of supramolecular structures, in which the molecules are arranged with their axes parallel to each other [1–5].

Polymers with a stiff helical rodlike structure have many advantages over other synthetic polymers because they often possess stable secondary structures due to cooperative intermolecular interactions. The α -helical secondary structure enforces a rodlike structure, in which the polypeptide main chain forms the inner part of the rod [6–8]. This rodlike feature is responsible for the formation of thermotropic and lyotropic liquid crystalline phases [9–13].

Incorporation of an elongated coillike block into the helical rod system in a single molecule is a unique way to create new supramolecular structures. The microstructures of rod–

* Corresponding author.

E-mail address: dsohn@hanyang.ac.kr (D. Sohn).

coil polymers arise from a combination of organizing forces including the immiscibility of the two blocks and the specific interactions between the rod blocks. Differences in the rod–coil ratio, which affects molecular packing and creates a thermodynamically stable microstructure, drive the formation of a variety of self-assembled microstructures such as lamellae, cylinders, micellar cubics, close-packed spheres, and disordered melts [14–16].

Semenov and Vasilenko (SV) initiated a theoretical study of the phase behavior of rod–coil block copolymers, in which they introduced four new terms: ideal gas entropy of mixing, steric interaction between rods, coil stretching, and unfavorable rod–coil interaction [17]. Muller and Schick (MS) also studied the phase behavior of rod–coil molecules by applying numerical self-consistent field theory within the weak segregation limit [18]. Their findings emphasized the importance of the conformational entropy of the flexible component. Though these studies provide valuable qualitative information about rod–coil block copolymers, they do not sufficiently improve the quantitative understanding of rod–coil block copolymer phase behavior.

Monolayers at the air–water interface provide an important and convenient model system for investigating the behavior of rod–coil copolymers [19–22]. When amphiphilicities are studied as Langmuir monolayers, the reduction in surface energy is expressed as the surface pressure, $\pi = \gamma_0 - \gamma$, where γ_0 and γ are the surface tensions of the clean water and monolayer-covered surfaces, respectively. Accordingly, pressure–area isotherms obtained by the surface film balance technique provide information about the stability and structure of the monolayer through experiments that change the temperature, pH, and other variables. In addition, the Langmuir–Blodgett (LB) technique allows the fabrication of ultrathin films through the deposition of monolayers from the air–water interface to solid substrates [23]. Indeed, LB films typically exhibit a high degree of orientational order that is induced at the water surface by two-dimensional geometrical restrictions.

The rod–coil molecule used in this study is poly(γ -benzyl-L-glutamate) (PBLG)–poly(ethylene oxide) (PEO) block copolymer. PBLG is hydrophobic, while PEO is hydrophilic [24]. PBLG is a synthetic polypeptide having a typical rigid α -helical conformation stabilized by hydrogen bonds. PBLG is soluble in several solvents due to favorable interactions between the solvent and the pendent benzyl side groups. The lyotropic liquid crystalline phases exhibited by PBLG have served as important model systems for rod-ordering theories of the liquid crystalline state. In addition, the interfacial behavior of PBLG and its derivatives has received a great deal of attention from researchers who wish to engineer functional surface arrays for electronics applications. Thus, PBLG is a useful model in the research of phase behavior of rigid polymers. In addition, PEO is one of the best-studied homopolymers, which forms a self-assembled structure by chain folding [25,26]. PEO is surface active, but it forms an insoluble monolayer despite being water-soluble

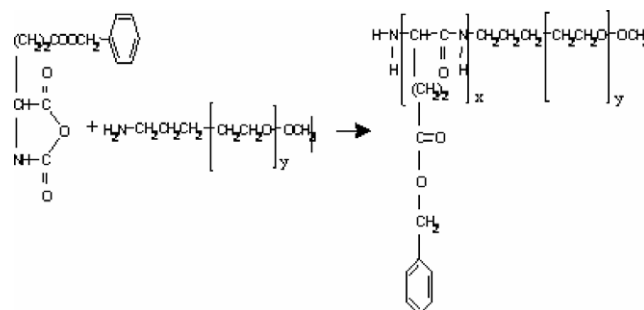


Fig. 1. Synthesis scheme of PBLG–PEO diblock copolymer.

at moderate temperatures in all proportions. PEO is a neutral and biodegradable polymer, so it is used for numerous biological and medical applications.

In this study, the monolayer behavior of PBLG–PEO diblock copolymers having the same PEO chains and different PBLG chain lengths at the air–water interface was investigated. Using pressure–area isotherms collected at different temperatures, the energy relationship between rod and coil as a function of rod length was examined [27–29]. In conjunction, the microstructures of these monolayers based on the energy relationship were investigated using AFM (atomic force microscopy).

2. Experiment

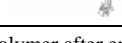
2.1. Materials

γ -Benzyl-L-glutamate N-carboxyanhydride (BLG–NCA) was prepared according to the method described by Goodman et al. [30]. Monoamine-terminated poly(ethylene oxide) (PEO, $M_w = 12,000$) was kindly supplied by Nippon Oil and Fat Co. The PBLG (poly(γ -benzyl-L-glutamate))–PEO (poly(ethylene oxide)) diblock copolymers were prepared by the ring-opening polymerization of BLG–NCA initiated with primary-amine-terminated PEO in methylene dichloride. The reaction scheme is shown in Fig. 1. PBLG–PEO block copolymer composition was estimated from the peak intensities of the NMR signal of methylene protons of the PBLG block (5.0 ppm) and the signal of the ethylene proton (3.6 ppm) of the PEO block. All of the block copolymers contained poly(ethylene oxide) of 273 monomers and poly(γ -benzyl-L-glutamate) part of 419, 182, and 38 monomers. The characteristics of the block polymer PBLG–PEO are summarized in Table 1. Chemical conformation and bulk properties of these polymers have been discussed in the previous paper [24].

2.2. Surface pressure measurement

The surface pressure–area isotherms were obtained using a film balance (KSV 3000) with a platinum Wilhelmy plate. Surface pressure–area isotherms were measured inside a Teflon trough mounted within a thermostatic cham-

Table 1
The molecular weight and the monomer ratio of GE-1, GE-2, and GE-3

Polymer	M_w^a	Monomer unit ratio ^b	PBLG	PEO ^c
GE-1	103,700	60.5:39.5		
GE-2	51,800	40.0:60.0		
GE-3	20,400	12.5:78.5		

Note. The pictures show the molecular models of each copolymer after energy minimization.

^a PEO M_w 12,000.

^b PBLG:PEO ratio obtained by the relative ratio of NMR signals.

^c Molecular modeling of PBLG–PEO after energy minimization.

ber. Subphase temperatures were maintained at 10, 20, and 30 ± 0.5 °C. The aqueous subphase was purified and deionized using a Millipore purification system (Milli-Q; resistivity 18.2 M Ω cm) equipped with an organic removal cartridge. Insoluble monolayers were prepared by dissolving copolymer samples in HPLC grade chloroform (Sigma-Aldrich Corporation) at concentrations ranging from 0.1 to 0.4 mg/ml. Samples of 80–150 μ l of solution were spread evenly over the water surface in small drops. After complete evaporation of the chloroform (about 20 min), the layer floating on the subphase was compressed symmetrically by two mobile barriers at a constant speed (7 mm/min). As measured by the compression–expansion scans, the solubility increases of these molecules on the air–water interface were negligible. Most surface pressure–area (π – A) isotherms were measured several times. Typical reproducibility for a given area was ± 0.2 mN/m.

2.3. Atomic force microscope (AFM) measurements

Monolayers on the water surface were deposited onto freshly cleaved mica substrates, which were pulled from the water while the film was compressing at a constant concentration (the vertical dipping method). The film was dried for about 20–30 min under ambient conditions. The samples were analyzed in noncontact mode with a commercial AFM (PSIA) equipped with microfabricated V-shaped silicon nitride cantilevers. The transfer of monolayers to the solid substrate did not introduce any artifacts. Microdomain dimensions were determined from top-view AFM images and data cross sections of these micrographs.

3. Result and discussion

3.1. Surface pressure–area isotherms

Surface pressure–area isotherms recorded for spread monolayers of GE-1, GE-2, and GE-3 are presented in Fig. 2. For GE-1, the first increase in surface pressure is noted at a surface area of 370 nm²/molec. The initial slope is moderate, but increases abruptly as the surface area becomes smaller than 175 nm²/molec, and dramatically increases

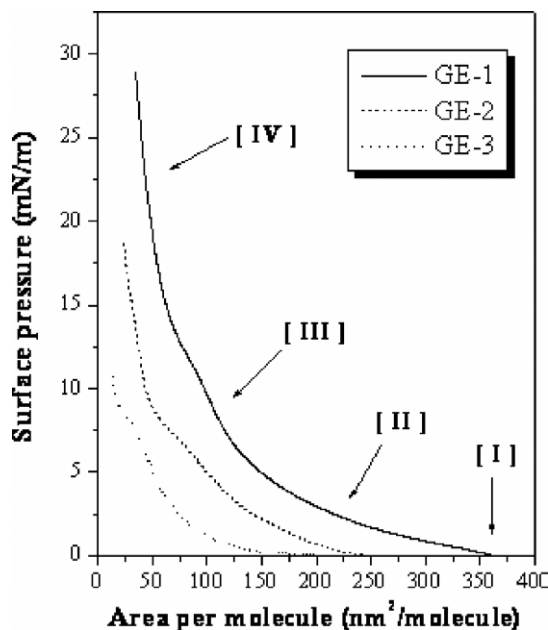


Fig. 2. Surface pressure–area isotherms of GE-1, GE-2, and GE-3 at the air–water interface: [I] gaseous, [II] liquid expanded, [III] liquid condensed, [IV] solid.

when the surface area becomes less than 100 nm²/molec. The three isotherms have similar shapes but the lift-off points are different. Upon compression, the PBLG isotherm curve of PBLG has plateau regions, due to the formation of a bilayer, which is one of the characteristic properties of a rigid rodlike polymer.

Malcolm reports that a cylindrical α -helical polypeptide monolayer on the water surface is composed of a number of individual molecules, which are formed from the lower layer and become nuclei for the formation of a second layer at the collapse pressure [31]. If the solid portion of the isotherm is extrapolated to zero surface pressure, the intercept gives the area per molecule that would be expected for the hypothetical state of an uncompressed close-packed layer. For BLG, the measured limiting area per residue was 0.197 nm² at 20 °C [32]. The pressure of the PEO monolayer increases slowly with a plateau occurring at 10 mN/m. This slow increase in surface pressure at low coverage is due to the increase of intermolecular interactions between the PEO molecules. After the formation of the PEO monolayer at the air–water interface, a PEO brush gradually forms in the long plateau region. The behavior of the monolayers of diblock copolymers consisting of PEO and PBLG at the air–water interface can be described by three desorption transitions. In region [I], the molecules freely move on the water surface. A slow increase [II] region is caused by the increasing intermolecular interaction of PEO. A gently increasing [III] region results from the gradually desorbed PEO block, which forms a brush. The sharp pressure increase [IV] region is attributed to a strongly compressed PEO brush and dominated by the intermolecular interaction of PBLG. Fig. 2 shows that GE-1 has a higher surface pressure than the other

Table 2

Comparison between extrapolated limiting area and supposed area of GE-1, GE-2, and GE-3

Polymer	Extrapolated area ^a (nm ²)	Supposed PBLG area ^b (nm ²)
GE-1	77.65	82
GE-2	67.18	35
GE-3	35.74	7.4

^a Extrapolated area was obtained from the π - A isotherm.

^b BLG area is 0.197 nm²/residue and the PEO area varied with compression at the air–water interface.

molecules at the same molecular area because of the bigger rods. The extrapolated limiting areas of GE-1, GE-2, and GE-3 from this graph are summarized in Table 2. Compared with these extrapolated limiting area of molecule and the calculated area of PBLG using BLG limiting area per residue, conformation transitions of molecules could be confirmed. If PEO were to collapse at about 10 mN/m, the extrapolated limiting area of GE-1, GE-2, and GE-3 would be equal to the calculated area of each PBLG rod. However, as shown in Table 2, the two values of GE-1 are similar, but the extrapolated limiting areas of GE-2 are approximately three times bigger than the calculated limiting area, and the extrapolated limiting area of GE-3 is even larger than the calculated limiting area. This may indicate that the degree of PEO desorption is affected by the length of the rod.

The monolayer compressibility (β) was determined at a constant temperature using the relationship

$$\beta = \frac{1}{A} \frac{dA}{d\pi} = \frac{d \ln A}{d\pi}, \quad (1)$$

where β is the compressibility, and A is the surface area [33].

Fig. 3 shows the compressibilities of the three monolayers and their normalized values. For example, it was estimated that β of the GE-3 monolayer is 0.73 m/mN at 10 mN/m at 20 °C. The magnitude of β indicates the degree of compression of the molecule. By using the normalized concentration (x -axis) we can neglect the effect of different molecular weights. GE-3 exhibits the highest compressibility among the three molecules. It is likely that GE-3 is more pliable than the other molecules. In other words, while the molecular weights of the hydrophilic coil parts are equal to each other, the degree of PEO desorption increases with rod length. This relationship is a major factor for the behavior of copolymer. As discussed in Introduction, the surface pressure, $\pi = \gamma_0 - \gamma$, where γ_0 and γ are the surface tensions of the clean water and monolayer covered surfaces, is another expression of the surface energy. By differentiating G with respect to A , at constant temperature and pressure, one can obtain

$$\gamma = \left(\frac{\delta G}{\delta A} \right) = \left(\frac{\delta H}{\delta A} \right) - T \left(\frac{\delta S}{\delta A} \right), \quad (2)$$

where G , H , S , A , T are Gibbs free energy, enthalpy, entropy, area per molecule, and temperature, respectively. Surface tension is the difference between cohesion and adhesion. The former refers to the interaction energy of the same

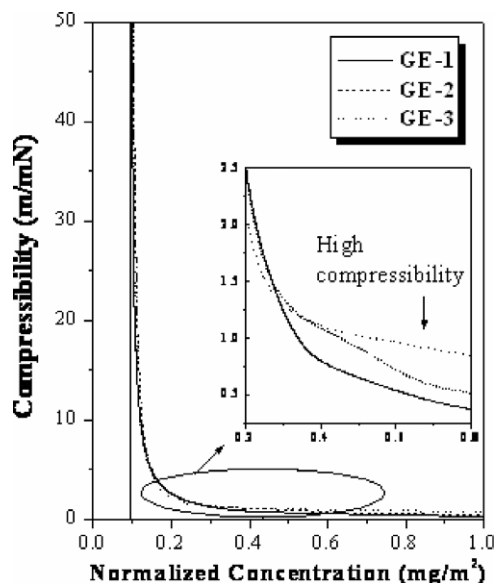


Fig. 3. Compressibility as a function of the normalized concentration of GE-1, GE-2, and GE-3 monolayers.

molecules and the latter refers to the interaction energy of different molecules. Therefore, surface tension can be an indicator of the energy relationship by the arrangement of molecules and can be analyzed quantitatively by the interaction between molecules. To investigate the effect of rod length on the PEO desorption, isotherm experiments were performed with the GE-1, GE-2, and GE-3 at various temperatures.

Fig. 4 shows the pressure–concentration isotherms of GE-1, GE-2, and GE-3 at 10, 20, and 30 °C. The isotherms for GE-1 and GE-2 exhibit two different regions. In the dilute region, where surface area concentration is low, π increases with increasing temperature. When surface area concentration is high, π decreases with increasing temperature. Unlike the shorter-tailed molecules, the GE-3 molecule with longer flexible tails does not show any transition.

In Fig. 5, the surface pressure at fixed surface concentration is plotted against temperature at four levels of surface coverage from 1.0 to 3.0 mg/m². There is a clear transition from slope $\delta\pi/\delta T > 0$, where

$$\frac{\delta\pi}{\delta T} = \frac{\delta(\gamma_0 - \gamma)}{\delta T}. \quad (3)$$

Thus, a positive temperature coefficient of surface pressure implies that surface tension of molecules decreases with increasing temperature. Thus, the adhesion free energy is greater than the cohesion free energy, and vice versa.

According to the Semenov and Vasilenco (SV) theory, the self-assembly of rod–coil copolymers is affected by intramolecular and intermolecular rod–coil interactions. The cohesion free energy consists of the rod–rod interaction energy and the chain–chain interaction, and the adhesion free energy consists of the incompatibility between rods and chains and the interaction between polymers and water. The interaction energy between polymer and water and the in-

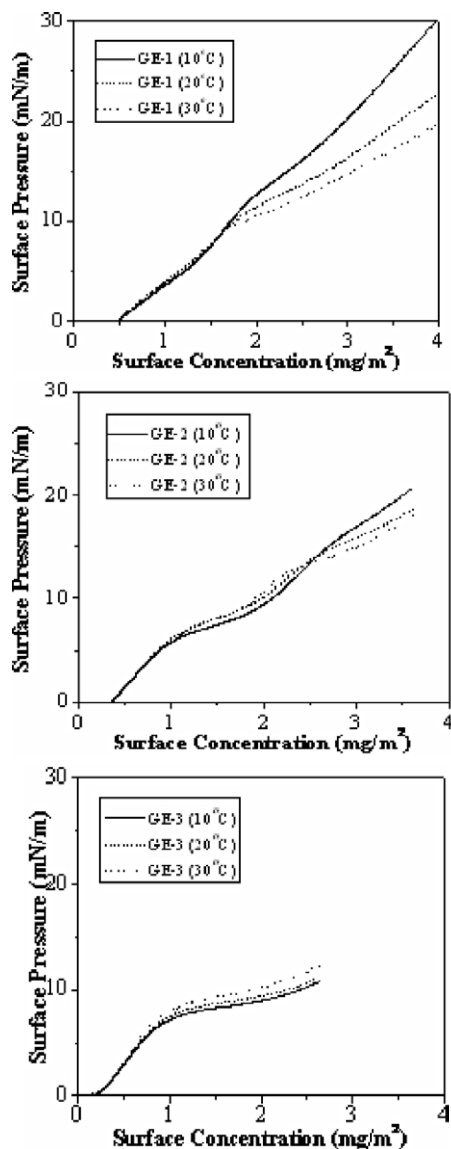


Fig. 4. Surface pressure plotted against surface concentration for GE-1, GE-2, and GE-3 at three temperatures (10 °C, solid line; 20 °C, dashed line; 30 °C, dotted line).

compatibility between rods and coils can be neglected because these are not affected by the molecular weight, but by the kind of molecule. Therefore, adhesion energy can be neglected. A positive temperature coefficient of surface pressure indicates a decrease in the surface tension. This means that the entropy decreases according to the increase of PEO stretching energy. On the other hand, a negative temperature coefficient of surface pressure indicates that surface tension of the monolayer increases. This means that the enthalpy decreases as the aggregation of PBLG rods increases. In conclusion, when the PEO stretching energy is greater than the PBLG packing energy, the temperature coefficient of surface pressure is positive. When the PBLG packing energy is greater than the PEO stretching energy, the temperature coefficient of surface pressure is negative. In the region where the packing energy and stretching energy cancel, PBLG and

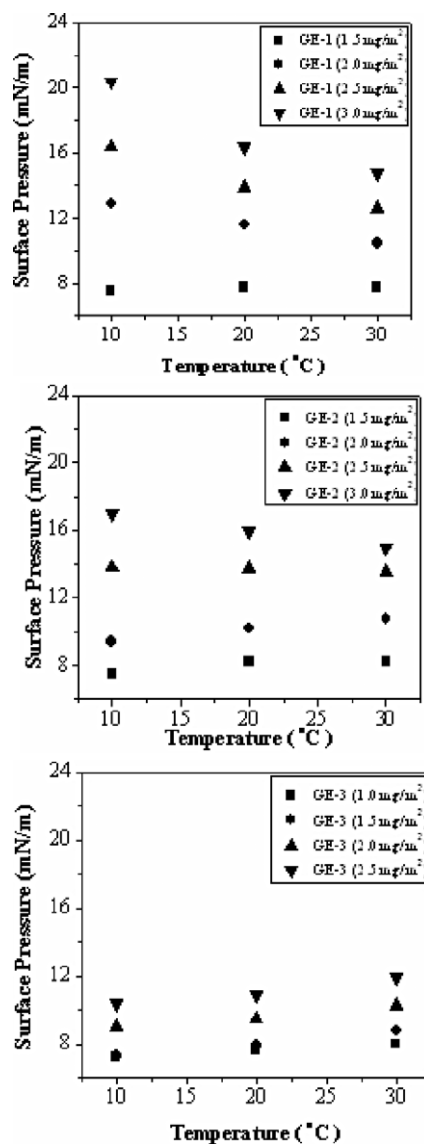


Fig. 5. Surface pressure vs temperature plots of (a) GE-1, (b) GE-2, and (c) GE-3 at various concentrations. (Unit of surface concentration is mg/m^2 .)

PEO show a transition point. This transition point is called the “setoff point,” which is governed by the rod and coil ratio. The GE-1 molecules with shorter flexible coils have a setoff point at $1.7 \text{ mg}/\text{m}^2$. The setoff point of GE-2 molecules is at concentration $2.5 \text{ mg}/\text{m}^2$, and the setoff point of the GE-3 molecule could not be observed because the PEO segment could not compress to the size of the rod segment.

3.2. Surface morphology by AFM

Fig. 6 shows atomic force microscopy (AFM) images for GE-1, GE-2, and GE-3 at low ($1.5 \text{ mg}/\text{m}^2$) and high concentrations ($2.5\text{--}3.0 \text{ mg}/\text{m}^2$). The positive temperature effect region occurs at the higher concentration and the negative temperature effect region occurs at the lower concentration.

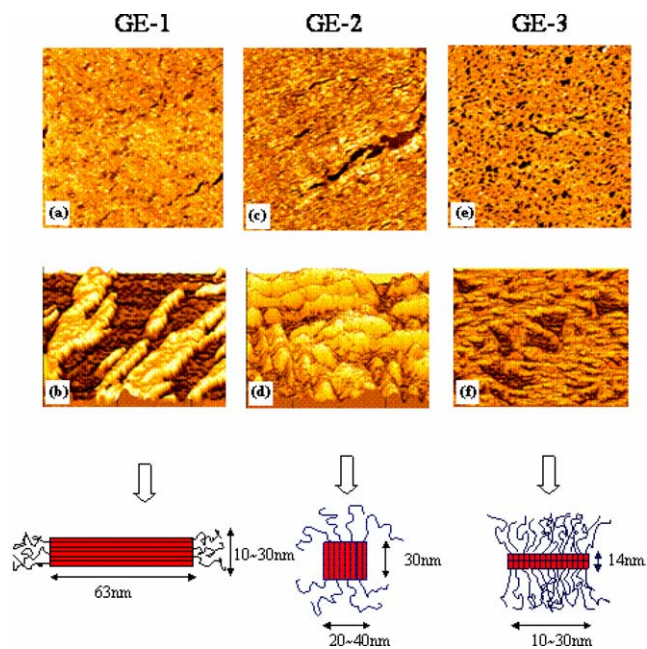


Fig. 6. AFM images of the PBLG–PEO monolayers film at different surface concentrations: (a) GE-1 at high concentration: (3.0 mg/m^2 , $5 \times 5 \mu\text{m}$), (b) GE-1 at low concentration (1.5 mg/m^2 , $250 \times 250 \text{ nm}$); (c) GE-2 at high concentration (3.0 mg/m^2 , $5 \times 5 \mu\text{m}$), (d) GE-2 at high concentration (1.5 mg/m^2 , $200 \times 200 \text{ nm}$); (e) GE-3 at high concentration (2.5 mg/m^2 , $5 \times 5 \mu\text{m}$), (f) GE-3 at low concentration (1.5 mg/m^2 , $250 \times 250 \text{ nm}$).

For GE-1 and GE-2 molecules, there is a void space similar to a bare subphase in the positive effect region because desorption of PEO was not complete. There is no void space in the negative temperature effect region. For GE-3, there are scattered void spaces in the 1.5 and 2.5 mg/m^2 concentration region. These results illustrate the effect of the rod-length-dependent packing energy of the PBLG–PEO copolymers. Molecules with longer rods were stabilized by the enthalpy reduction of rod packing. Molecules with shorter rods have a relatively small enthalpy decrease due to rod packing and large entropy decrease due to coil repulsion. Therefore, microstructures of PBLG–PEO molecules suggest competition between entropic loss resulting from the PEO repulsion and enthalpic decrease due to PBLG packing. These energy relationships are key factors that govern the microstructure of rod–coil molecules.

The observed morphologies of the molecules differ due to their block composition. The transferred GE-1 at surface concentration 1.5 mg/m^2 , which is the region of positive temperature effect, forms cylindrical micelles with average lengths $63 \pm 2 \text{ nm}$ and widths $12 \pm 2 \text{ nm}$. The rod blocks were tightly packed in the region of negative temperature coefficient of GE-1 at 3.0 mg/m^2 . For GE-2, in the positive temperature effect region, circular micelles were observed with a distance between the length of $30 \pm 2 \text{ nm}$ and the width of $30 \pm 2 \text{ nm}$. In the negative temperature effect region, the morphology of GE-2 is similar to that of GE-1. For GE-3, in the 1.5 and 30 mg/m^2 regions, the monolayer is perforated with many holes.

As shown in Fig. 6, at low surface pressure, GE-1 and GE-2 have large domains where the deduced size of the domains is the same as that of the rod block of the molecule and the contribution of the coil block is negligible. It is estimated that a single aggregate contains 10–30 molecules, which are hypothesized have to a “monolayer puck” structure proposed by Fredricson for the bulk structure [34]. But the length of the rod of GE-3, $\sim 14 \text{ nm}$, in the AFM image is different from the calculated rod length, $\sim 7 \text{ nm}$. Based on these experimental observations, one can estimate bilayer structure. According to the Fredricson model, molecules with long chains form the puck micelle structure. But as in Table 2, the size of the EO monomer unit in a two-dimensional system is about $15\text{--}20 \text{ \AA}^2$. The size of the calculated coil of GE-3 is about $15\text{--}20 \times 273 = 4095\text{--}5460 \text{ \AA}^2$, but the rod size of GE-3 is $\sim 7 \text{ nm}$ [35]. Thus, for PEO stretching in the GE-3 system there is no difference between the bilayer and micellar puck structures. Thus, when the GE-3 molecular forms a structure such as the bilayer, it compensates for the enthalpy decrease by rod packing.

In summary, we analyzed the self-organization of rod–coil diblock copolymer into microstructures through surface pressure isotherm analysis. The results show that the energy relationship of PBLG–PEO diblock copolymer is a competition between entropy loss of the PEO aggregation and enthalpy decrease of the PBLG packing. When the enthalpy decrease of the PBLG packing is smaller than the entropy loss, the surface pressure has a positive temperature coefficient. When the enthalpy decrease of the PBLG packing is greater than the entropy loss, the observed surface pressure has a negative temperature coefficient. In the low-concentration region, entropy loss of the PEO stretching is larger, and in the observed high-concentration region, enthalpy decrease of the PBLG packing is larger. In addition, the setoff points, where the enthalpy and entropy losses cancel each other, are different depending on the rod and coil ratio. This means that the longer rod molecules have a bigger enthalpy decrease, so the setoff point appears in the area of lower concentration.

The enthalpy effect of rod packing influences the microstructures at the air–water interface. GE-1, with the long rods, forms a cylindrical structure in the monolayer due to the bigger enthalpy decrease. GE-2, with the middle-sized rods, forms micellar structure in the monolayer by self-assembly. GE-3, with the short rods, forms a bilayer structure in the monolayer and clusters with nodal self-assembly. These results demonstrate that the microstructures of PBLG–PEO diblock copolymers are related to energy differences between rods and the coil block.

Acknowledgments

This work has been supported by the research fund from KOSEF (Grant No. R-14-2002-004-01002-0) and Y. Park thanks Nano Science and Technology in Korea (KISTEP) for their support.

References

- [1] K. Yu, A. Eisenberg, *Macromolecules* 31 (1998) 3509.
- [2] J. Kim, S.K. McHugh, T.M. Swager, *Macromolecules* 32 (1999) 1500.
- [3] M. Lee, B.K. Cho, Y.G. Jang, W.C. Zin, *J. Am. Chem. Soc.* 122 (2000) 7449.
- [4] A.J. Williams, V.K. Gupta, *J. Phys. Chem. B* 105 (2001) 5223.
- [5] S. Lecommandoux, M.F. Achard, J.F. Langenwalter, H.A. Klok, *Macromolecules* 34 (2001) 9100.
- [6] J. Watanabe, H. Ono, *Macromolecules* 19 (1986) 1079.
- [7] M. Kawaguchi, M. Yamamoto, N. Kurauchi, T. Kato, *Langmuir* 15 (1999) 1388.
- [8] R. Tadmor, Y. Cohen, R.L. Khalfin, *Langmuir* 18 (2002) 7146.
- [9] S. Machida, T.I. Urano, K. Sano, Y. Kawata, K. Sunohara, H. Sasaki, M. Yoshiki, Y. Mori, *Langmuir* 11 (1995) 4838.
- [10] J. Stumpe, T. Fischer, H. Menzel, *Macromolecules* 29 (1996) 2831.
- [11] D.L. Koch, O.G. Harlen, *Macromolecules* 32 (1999) 219.
- [12] S. Schmidtke, P. Russo, J. Nakamatsu, E. Buyuktanir, B. Turfan, E. Temyanko, I. Negulescu, *Macromolecules* 33 (2000) 4427.
- [13] S.M. Yu, C.M. Soto, D.A. Tirrell, *J. Am. Chem. Soc.* 122 (2000) 6552.
- [14] M. Lee, B.K. Cho, H. Kim, J.Y. Yoon, W.C. Zin, *J. Am. Chem. Soc.* 120 (1998) 9168.
- [15] M. Sayar, S.I. Stupp, *Macromolecules* 34 (2001) 7135.
- [16] M. Reenders, G. ten Brinke, *Macromolecules* 35 (2002) 3266.
- [17] A.N. Semenov, S.V. Vasilenko, *Sov. Phys. JETP* 63 (1986) 70.
- [18] M. Muller, M. Schick, *Macromolecules* 29 (1996) 1091.
- [19] V.B. Fainerman, D. Vollhardt, *J. Phys. Chem. B* 103 (1999) 145.
- [20] M.C. Faure, P. Bassereau, M.A. Carignano, I. Szleifer, Y. Gallot, D. Andelman, *Eur. Phys. J. B* 3 (1998) 365.
- [21] M. Kawaguchi, M. Yamamoto, T. Nakamura, M. Yamashita, T. Kato, *Langmuir* 17 (2001) 4677.
- [22] Y. Seo, J.H. Im, J.S. Lee, J.H. Kim, *Macromolecules* 34 (2001) 4842.
- [23] N.H. Lee, L.M. Christensen, C.W. Frank, *Langmuir* 19 (2003) 3525.
- [24] C.S. Cho, J.W. Nah, Y.I. Jeong, J.B. Cheon, S. Asayama, H. Ise, T. Akaike, *Polymer* 40 (1999) 6769.
- [25] A. Wesemann, H. Ahrens, R. Steitz, S. Forster, C.A. Helm, *Langmuir* 19 (2003) 709.
- [26] E.E. Dormidontova, *Macromolecules* 35 (2002) 987.
- [27] J. Daniel, S.G. Kuzmenka, *Macromolecules* 21 (1988) 779.
- [28] M. Mabuchi, S. Ito, M. Yamamoto, T. Miyamoto, A. Schmidt, W. Knoll, *Macromolecules* 31 (1998) 8802.
- [29] H. Yim, M.D. Foster, J. Engelking, H. Menzel, A.M. Ritcey, *Langmuir* 16 (2000) 9792.
- [30] W.D. Fuller, M.S. Verlander, M. Goodman, *Biopolymers* 15 (1976) 869.
- [31] R.R. Malcolm, in: *Progress in Surface and Membrane Science*, vol. 7, Academic Press, New York, 1974, p. 183.
- [32] A. Shibata, S. Ueno, Y. Ito, S. Yamashita, *Langmuir* 14 (1998) 7519.
- [33] A. Angelova, R. Ionov, *Langmuir* 15 (1999) 7199.
- [34] D.R.M. Williams, G.H. Fredrickson, *Macromolecules* 25 (1992) 3561.
- [35] E.E. Dormidontova, *Macromolecules* 35 (2002) 987.